

Fermented grape pomace ash – by-product of rakia (brandy) production

Aleksandar Nikolov*, Liliya Tsvetanova, Borislav Barbov, Ivan Tsanev, Yana Tzvetanova

Institute of Mineralogy and Crystallography, Bulgarian Academy of Sciences, Acad. G. Bonchev Str., bl. 107, 1113 Sofia, Bulgaria;

*drsashko@imc.bas.bg

Abstract: This study investigates the chemical, mineralogical, and functional characteristics of fermented grape pomace ash generated after brandy production and subsequent combustion. Semi-quantitative WDXRF analysis revealed a Ca–K–P-dominated composition with high alkalinity, significant phosphorus content, and notable copper concentration. The water-soluble fraction of the ash was determined to be 17.1 wt.%, indicating a moderate content of mobile inorganic salts that may influence leaching behaviour and environmental compatibility. XRD and vibrational spectroscopy confirmed the presence of lime, calcite, silicates, sulphates, and calcium phosphate phases, including hydroxyapatite, together with a significant amorphous fraction and residual carbon. UV–Vis analysis indicated partial reduction of copper species to metallic nanoparticles, suggesting heterogeneous redox conditions during thermal treatment. The combined composition confers potential functionality in soil amendment, mineral carbonation for CO₂ sequestration, and incorporation into cementitious or alkali-activated systems, although soluble salts and copper mobility represent critical constraints, requiring application-specific environmental and performance assessment.

Keywords: FERMENTED, GRAPE, POMACE, ASH, CHARACTERIZATION, BY-PRODUCT

1. Introduction

The wine and spirits industries generate substantial quantities of solid by-products, among which grape pomace represents the dominant fraction by mass. Grape pomace, consisting of skins, seeds, and varying amounts of stalks, accounts for approximately 20–30 wt.% of processed grapes and is produced continuously and seasonally in large volumes [1-3]. While numerous valorisation pathways for fresh or dried grape pomace have been explored, primarily in the food, feed, and nutraceutical sectors [4,5], the management of pomace residues following alcoholic fermentation and distillation remains comparatively underexplored. In particular, solid residues generated after brandy production are often treated as low-value waste streams, despite undergoing substantial physicochemical transformation during fermentation.

Alcoholic fermentation induces pronounced changes in grape pomace composition through the consumption of fermentable sugars, partial degradation of polysaccharides, redistribution of organic acids, and mobilization of inorganic species. Studies focusing on the chemical and nutritional composition of grape pomace consistently show that its mineral fraction is dominated by potassium, calcium, phosphorus, and magnesium, with variability arising from grape variety, processing route, and presence of stalks [1,2,5]. However, these studies primarily address unfermented or food-grade pomace, where the organic matrix remains largely intact.

Thermochemical utilization of grape pomace has been investigated mainly in the context of energy recovery. Combustion and pyrolysis studies demonstrate that grape pomace exhibits high ash content and a mineral composition prone to alkali-related challenges such as slagging, fouling, and ash deposition [6]. Mortari et al. [8] showed that water-soluble inorganic constituents, particularly potassium, significantly influence combustion behaviour and char reactivity, while Moço et al. [7] reported severe ash deposition and sintering during high-temperature combustion of pulverized grape pomace. These findings underline the strong influence of inorganic matter on the thermal behaviour of pomace-derived materials but remain focused on fuel performance, rather than on the properties or potential applications of the resulting ash.

From a resource-efficiency and circular-economy perspective, biomass ashes have attracted increasing attention as secondary raw materials in construction, agriculture, and environmental applications [8]. Depending on their oxide composition and mineralogical assemblage, ashes may exhibit alkalinity, nutrient value, or reactive phases suitable for soil amendment, stabilization processes, or incorporation into cementitious systems [9]. Given the high contents of calcium, potassium, phosphorus, and silica reported for grape pomace and its fractions [3], fermented grape pomace ash may offer functional properties extending beyond

energy-related considerations. However, without systematic chemical and mineral characterization, such potential applications remain speculative.

The specific aim of this work is to characterize fermented grape pomace ash and to assess its potential applications in value-added domains. By linking elemental composition and mineralogical features to plausible functional uses, this study contributes to the broader understanding of grape pomace-derived residues within sustainable material cycles, while explicitly recognizing the influence of local feedstock variability and processing conditions.

2. Materials and methods

2.1. Materials

The grape variety used for fermentation was the black Otel from the area of Zemen, Bulgaria, vintage 2024). The grapes exhibited an initial sugar content of about 20%, determined in situ using a handheld refractometer. The grape was mechanically crushed using a manual machine. The resulting mixture of liquid, seeds, skins and stalks was used as the fermentation feedstock. An additional 15–20 wt.% sugar solution was added to the fermenting mass in order to adjust the consistency and enhance alcohol yield. Fermentation was carried out in plastic barrels at a controlled temperature of 22 °C. To ensure process homogeneity, the fermenting mass was mixed daily. After approximately three weeks, the sugar content decreased to zero, indicating completion of fermentation.

The fermented material was subsequently transferred to a 120 L traditional copper distillation unit, operated using wood as the heat source, where alcohol was extracted. The residual solid matter remaining after distillation was mechanically dewatered using a screw press and subsequently formed into briquettes with approximate dimensions of 16×8×5 cm using a manual press (Fig. 1). The briquettes were placed on an outdoor shelf under a roof and allowed to dry. The briquette was burned into wood stove (Tim Systems, Serbia, efficiency 79%) and the obtained ash was examined.



Fig. 1. Dried briquette produced from pressed fermented grape pomace.

2.2. Methods

The elemental composition of the provided samples was determined using a Supermini200 spectrometer (Rigaku, Japan). Measurements were performed by wavelength-dispersive X-ray fluorescence (WDXRF) at an operating voltage of 50 kV and a current of 4.00 mA. Data processing was conducted using the ZSX software package. Samples were placed in a holder with an irradiated area of 30 mm in diameter. Before analysis, the samples were ground and pressed using a binder (Acrawax C powder) at a sample-to-binder ratio of 5:1 (w/w). A semi-quantitative method (SQX) was employed to determine elemental composition.

Powder X-ray diffraction analysis was performed on Empyrean (Malvern Panalytical, Almelo, The Netherlands) diffractometer equipped with a PIXcel3D detector and copper X-ray source (CuK α = 1.5406 Å). At 40 kV and 30 mA.

UV-Vis reflectance spectra were recorded using a Cary 4000 spectrophotometer (Agilent Technologies) equipped with an internal DRA 900 diffuse reflectance accessory (IMC-BAS). Transmittance spectra were additionally recorded using a solid sample accessory. Measurements were performed in the 200–800 nm spectral range with a spectral resolution of 1 nm. Baseline fluctuations were corrected prior to analysis. The diffuse reflectance data were converted to absorbance using the Kubelka-Munk function $F(R)$

Fourier-transform infrared (FTIR) spectra were collected on a Bruker Tensor 37 spectrometer in the spectral range 4000 - 400 cm^{-1} (IMC-BAS). The measurements were performed on powdered samples KBr pellet. Each spectrum represented the average of 128 scans, ensuring an enhanced signal-to-noise ratio and improved spectral resolution.

Raman measurements were carried out using an alpha300 R confocal Raman microscope (WITec) equipped with a 532 nm excitation laser (IMC-BAS). Spectra were recorded using $\times 10$ and $\times 50$ objectives. The spectral range covered approximately 100–3200 cm^{-1} .

The water-soluble fraction was determined by suspending oven-dried ash (80 °C) in distilled water at a solid-to-liquid ratio of 1:20 (w/v). The suspension was maintained under static conditions for 48 h with intermittent manual stirring to promote dissolution. Subsequently, the mixture was filtered, and the filtrate was collected and evaporated to dryness at 80 °C to recover the dissolved solids. The water-soluble content was calculated as the mass ratio of the recovered solid residue to the initial dry mass of the ash.

3. Results and Discussion

3.1. Water-soluble content

The water-soluble content of the fermented grape pomace ash was determined to 17.1 wt.%. This value falls within the broad range reported for biomass ashes (1–60.0 wt.%), but it is lower than the mean value summarized for various agricultural and woody biomass ashes combusted at 500 °C [10]. According to the review data, biomass ashes commonly exhibit significantly higher water-soluble fractions than the corresponding raw biomasses due to the formation of alkali chlorides, sulphates, and carbonates during combustion. The measured 17.1 wt.% therefore indicates moderate enrichment in water-soluble salts, suggesting partial development of such phases but lower overall salt accumulation compared to highly K-type or salt-tolerant biomasses described in the literature [10].

From a materials perspective, this fraction is critical because it controls alkalinity, leaching behaviour, and potential reactivity, and thus directly influences both technological performance and environmental compatibility of the ash. The solid residue was analyzed also in next section (referred as 'washed').

3.2. Chemical composition

The semiquantitative WDXRF analysis (Table 1) shows that the fermented grape pomace ash is predominantly composed of CaO (34.9 wt%) and K₂O (29.7 wt%), followed by significant P₂O₅ (16.3 wt%). Secondary components include MgO (5.03 wt%) and SiO₂ (5.23 wt%), while SO₃ (3.34 wt%), CuO (2.12 wt%), Al₂O₃ (1.50 wt%), and Fe₂O₃ (1.48 wt%) occur in lower concentrations. The dominance of CaO and K₂O indicates that the ash is strongly alkaline, consistent with the high mineral content typical of grape pomace residues reported in the literature (olive pomace and wine stillage studies show high ash fractions and mineral content in distillation by-products) [11]. Calcium in grape residues is largely derived from skins and seed material, where it serves as a structural component of cell walls. Upon combustion, organically bound calcium is converted primarily to CaO and CaCO₃ phases, consistent with the strong alkaline character observed in other biomass ashes and their high neutralizing potential. Potassium, which is highly mobile in plant tissues, becomes relatively concentrated during fermentation and subsequent distillation of grape pomace. Although literature on XRD phases in grape pomace ash is limited, biomass ash studies generally report calcium carbonates, alkali sulphates, silicates, and other mineral phases depending on the feedstock. The presence of phosphate phases such as Ca₅(PO₄)₃(OH), suggested by the P₂O₅ content, aligns with known thermal transformations of P-rich biomasses during combustion, favoring the formation of calcium phosphate minerals that are agronomically relevant. In condensed combustion residues of biomass ashes, these phosphate phases often occur alongside silicates and carbonates in ashes with high Ca and P content [12].

Table 1. Semi-quantitative chemical composition of the Fermented Grape Pomace Ash, determined by WDXRF (in wt.%).

Component	Fermented grape pomace ash	Fermented grape pomace ash after washing
MgO	5.03	6.37
Al ₂ O ₃	1.50	1.57
SiO ₂	5.23	6.70
P ₂ O ₅	16.30	17.40
SO ₃	3.34	0.15
Cl	0.103	0.015
K ₂ O	29.70	14.80
CaO	34.91	45.60
MnO	0.14	0.23
Fe ₂ O ₃	1.48	2.81
CuO	2.12	3.50
Others	0.132	0.132

The moderate SiO₂ content and trace microelements (Cu, Zn, Mn) reflect the intrinsic mineral profile of grape biomass, which contains significant amounts of macronutrients such as K, Ca, P, and Mg in the raw pomace matrix before combustion, consistent with comprehensive characterisation studies of grape waste materials [13].

Compared with raw grape pomace and distillation stillage compositions reported in recent studies, the fermented grape pomace ash shows an enriched inorganic profile due to calcination and also the depletion of organic matter through fermentation and distillation, resulting in higher relative concentrations of ash-forming elements [11]. This trend highlights that fermented grape pomace ash is a chemically distinct material, characterised by high

alkalinity and significant Ca–K–P content, differentiating it from ashes derived from raw or minimally processed pomace.

The substantial P_2O_5 content of 16.3 wt% is particularly noteworthy. Phosphorus, initially present in both organic and inorganic forms within grape seeds and skins, becomes concentrated during combustion, leading to the formation of phosphate-bearing mineral phases. The combined presence of CaO and P_2O_5 suggest the possible formation of calcium phosphate phases, which are relevant for agronomic applications where slow phosphorus release is desired. The coexistence of MgO further supports the potential formation of mixed Ca–Mg phosphate phases or discrete MgO units. SiO_2 content is moderate compared with typical lignocellulosic biomass ashes but may derive from intrinsic plant silica and minor extrinsic contamination.

The CuO content (2.12 wt.%) is notably high for typical biomass ash and likely reflects an anthropogenic origin. A primary source is the application of Bordeaux mixture ($CuSO_4 + Ca(OH)_2$) in vineyards, leading to copper accumulation in grape tissues and residues [14]. An additional contribution may arise from copper distillation equipment, where acidic fermentation media can promote Cu leaching and subsequent incorporation into the solid fraction.

Overall, the oxide and mineralogical composition indicate that fermented grape pomace ash is a calcium–potassium-rich alkaline ash with considerable phosphorus content, suggesting functional relevance for agricultural (e.g., soil amendment, slow-release P source), environmental, and construction-related applications.

3.3. Mineral Composition

The principal crystalline phases identified in the fermented pomace ash were lime (CaO), calcite ($CaCO_3$), quartz (SiO_2), anorthite ($CaAl_2Si_2O_8$), arcanite (K_2SO_4), periclase (MgO), and hydroxyapatite ($Ca_5(PO_4)_3OH$) (Fig. 2). The coexistence of free lime and calcite and also potassium-calcium carbonate suggests secondary carbonation processes, either during cooling inside the kiln (reaction of CaO/ K_2O -bearing phases with CO_2 in the flue gases) or through subsequent atmospheric weathering during storage. Given the high reactivity of free CaO and alkali oxides, rapid CO_2 uptake is thermodynamically favoured under ambient conditions, especially in the presence of hygroscopic phases such as arcanite [15].

The identification of anorthite indicates interaction between Ca-rich phases and aluminosilicate components at elevated temperature, implying partial solid-state reactions within the ash matrix. Periclase likely originates from Mg-bearing organic or soil-derived inputs, while hydroxyapatite reflects the concentration of phosphorus in grape residues.

A pronounced amorphous halo is observed in the 25–35° 2 θ range, indicating the presence of a substantial non-crystalline or poorly ordered phase fraction. In biomass-derived ashes, such a diffuse scattering feature is typically associated with amorphous aluminosilicate or siliceous glassy phases formed during combustion. The position of the halo suggests a silica-rich amorphous phase, potentially incorporating Ca, K, and Mg as network modifiers. The presence of amorphous phase may strongly influence the material's reactivity, particularly under alkaline activation or carbonation conditions.

3.4. Optical and Vibrational Characterization

Optical and vibrational spectroscopy were employed to refine the structural interpretation derived from XRF and XRD analyses and to clarify copper speciation, phosphate organization, and carbon structural ordering within the ash matrix. While XRF provides bulk

compositional data and XRD identifies dominant crystalline phases, spectroscopic techniques enable evaluation of bonding environments, structural substitutions, and redox-related transformations.

3.4.1. UV–Vis diffuse reflectance analysis

The UV–Vis diffuse reflectance spectrum of the ash, expressed using the Kubelka-Munk function $F(R)$, exhibits a distinct absorption band centered at approximately 566 nm (Fig. 3). This band falls within the characteristic range (~540–580) reported for localized surface plasmon resonance of metallic copper (Cu^0) nanoparticles, reflecting collective electron oscillations in zero-valent copper domains [16].

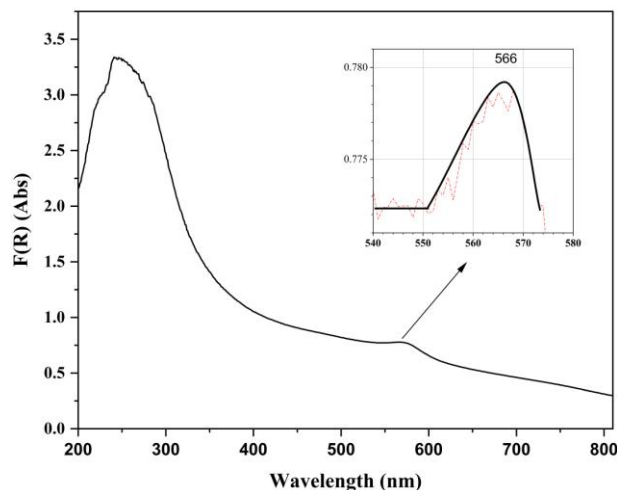


Fig. 3. UV–Vis diffuse reflectance spectrum of copper-containing fermented grape pomace ash recorded in the 200–800 nm range and presented as the Kubelka–Munk function $F(R)$. A surface plasmon resonance (SPR) band centred at approximately 566 nm indicates the presence of metallic copper nanoparticles.

Considering the copper concentration exceeding 2 wt.% (expressed as CuO equivalent) established in Section 3.1, the presence of a plasmonic response indicates that a fraction of copper is present in reduced metallic form. XRD analysis suggests possible copper oxide phases; however, peak overlap prevents unambiguous phase identification. UV Vis spectroscopy therefore provides complementary information regarding copper speciation that cannot be resolved solely through bulk or crystallographic techniques.

The relatively broad character of the plasmon band suggests nanoscale dispersion and interaction with the surrounding phosphate–carbonate matrix. The occurrence of metallic copper is consistent with partial redox transformation of Cu^{2+} species during combustion. The presence of residual carbon domains, confirmed by Raman spectroscopy, supports the plausibility of localized reducing microenvironments facilitating this transformation.

The XRF analysis indicates a copper content exceeding 2 wt.% (expressed as CuO equivalent), confirming the significant presence of copper within the ash. While XRF provides bulk elemental composition, it does not differentiate between oxidation states. The detection of an LSPR band in the visible region suggests that part of the copper is present in reduced metallic form.

The formation of metallic copper nanoparticles may be attributed to partial reduction of Cu^{2+} species during combustion under locally reducing conditions created by residual carbonaceous matter. Such microenvironments are consistent with the Raman evidence of disordered carbon structures.

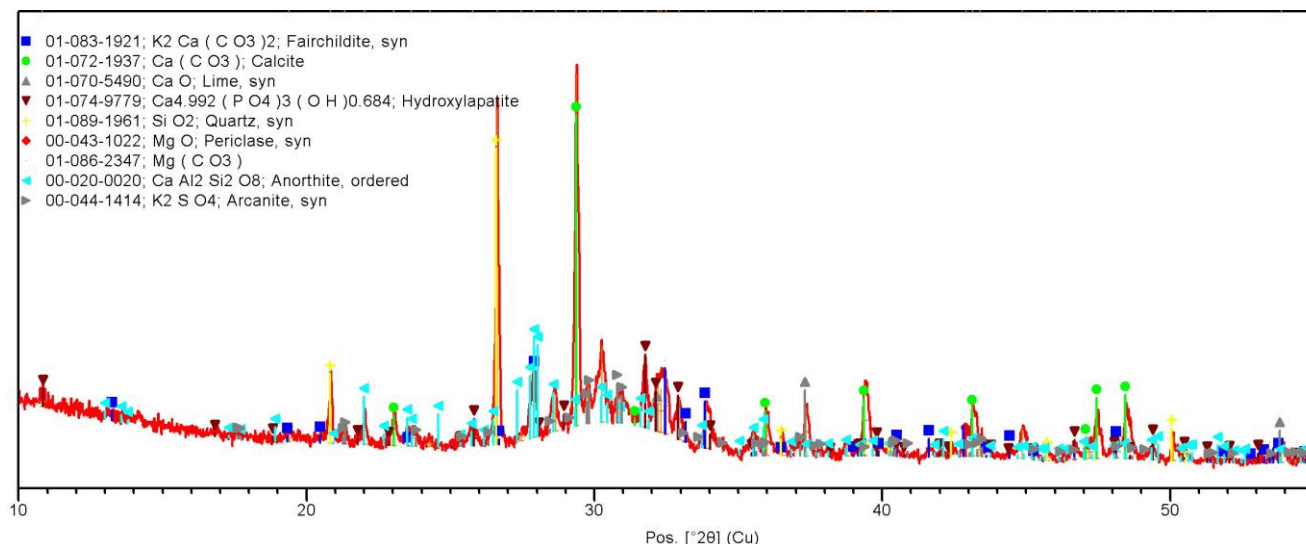


Fig. 2. Powder XRD pattern of fermented grape pomace ash.

3.4.2. FTIR spectroscopy

FTIR spectroscopy was employed to resolve bonding environments within the mineral matrix and to complement the structural interpretation derived from XRD and Raman analyses. The spectrum recorded in the 4000 - 400 cm^{-1} region exhibits several well-defined absorption bands indicative of a phosphate-carbonate dominated ash composition (Fig. 4).

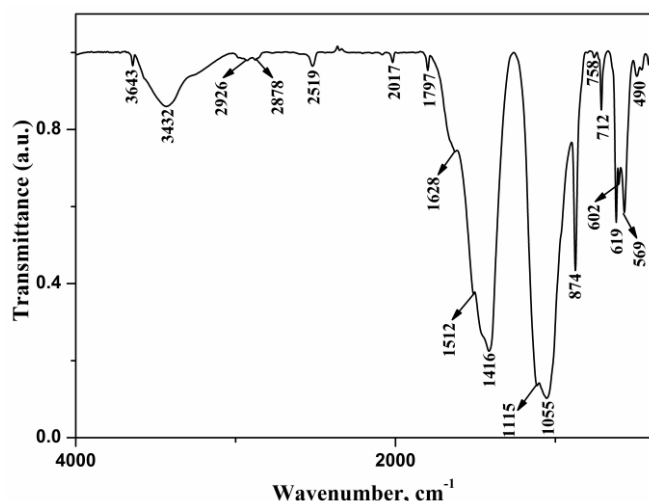


Fig. 4. FTIR spectrum of fermented grape pomace ash. Characteristic absorption bands corresponding to phosphate (PO_4^{3-}), carbonate (CO_3^{2-}), and hydroxyl groups are observed.

A broad band centered near $\sim 3432 \text{ cm}^{-1}$ is attributed to O-H stretching vibrations associated with adsorbed moisture and structural hydroxyl groups, while weak features around 2926 and 2878 cm^{-1} suggest minor residual organic C-H stretching. The band at $\sim 1628 \text{ cm}^{-1}$ corresponds to H-O-H bending of adsorbed water [17].

The mid-infrared region is dominated by strong absorptions at ~ 1115 and $\sim 1055 \text{ cm}^{-1}$, assigned primarily to ν_3 asymmetric stretching vibrations of PO_4^{3-} groups, with possible overlap from Si-O-Si stretching, indicating coexistence of phosphate and minor silicate components [18,19]. A distinct band at $\sim 874 \text{ cm}^{-1}$ together with bands near ~ 712 and $\sim 1416 \text{ cm}^{-1}$ confirms the presence of carbonate groups (CO_3^{2-}), consistent with calcite formation and/or carbonate substitution within the apatite lattice [20].

Additional bands observed at ~ 602 and $\sim 569 \text{ cm}^{-1}$ correspond to ν_4 bending modes of PO_4^{3-} , providing strong evidence for apatite-type calcium phosphate phases. Weak features below 500

cm^{-1} may reflect lattice vibrations of mixed Ca-O and phosphate frameworks. No clearly resolved Cu-O vibrational bands were identified, likely due to spectral overlap with phosphate modes and the relatively low or dispersed copper fraction inferred from complementary analyses.

Overall, the FTIR data corroborate a calcium phosphate-carbonate mineral framework with minor silicate contributions and hydrated surface functionalities. These findings are consistent with Raman and XRD results and support the interpretation of a partially carbonated apatite matrix hosting dispersed copper species within a thermally transformed biogenic ash.

3.4.3. Raman spectroscopy

The Raman spectrum of the mineral fraction is dominated by an intense band at 952 cm^{-1} corresponding to the ν_1 symmetric stretching mode of PO_4^{3-} , which is characteristic of apatite-type calcium phosphates (Fig. 5). Additional phosphate-related vibrations are observed at 433 cm^{-1} (ν_2 bending) and at 587 cm^{-1} (ν_4 bending), confirming the presence of a crystalline phosphate framework [21].

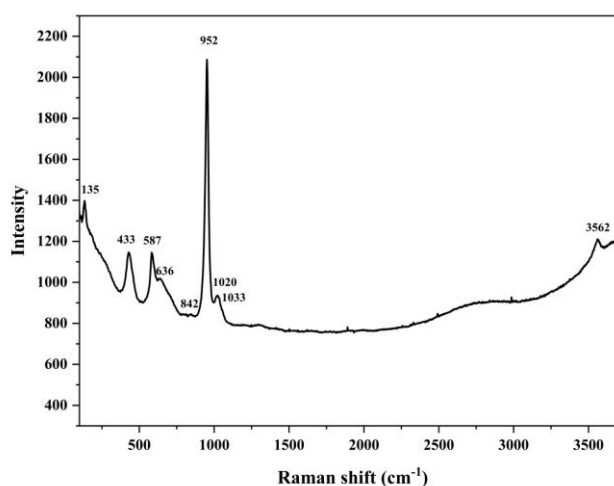


Figure 5 Raman spectrum of the mineral fraction of fermented grape pomace ash, showing a dominant band at $\sim 960 \text{ cm}^{-1}$ assigned to the ν_1 symmetric stretching mode of PO_4^{3-} .

A band at 636 cm^{-1} is assigned to librational vibrations of structurally bound hydroxyl groups, while a distinct sharp peak at 3562 cm^{-1} corresponds to the $\nu(\text{OH}^-)$ stretching mode [21]. The simultaneous presence of these two hydroxyl-related Raman

features provides strong spectroscopic evidence for hydroxyapatite rather than anhydrous calcium phosphate phases.

Additional bands at 1020 and 1033 cm^{-1} are attributed to ν_3 asymmetric stretching modes of PO_4^{3-} , and a feature at 842 cm^{-1} may indicate carbonate substitution within the apatite lattice [22].

Overall, the Raman data confirm that the dominant mineral phase corresponds to hydroxyl-containing, partially carbonated apatite structures, in agreement with XRD and FTIR results.

Raman spectra of carbonaceous inclusions exhibit D ($\sim 1350\text{ cm}^{-1}$) and G ($\sim 1590\text{ cm}^{-1}$) bands typical of disordered sp^2 carbon (Fig. 6). The estimated intensity ratio ($\text{ID}/\text{IG} \approx 0.8$) indicates partially ordered but predominantly amorphous carbon, characteristic of thermally transformed lignocellulosic biomass under non-ideal combustion conditions

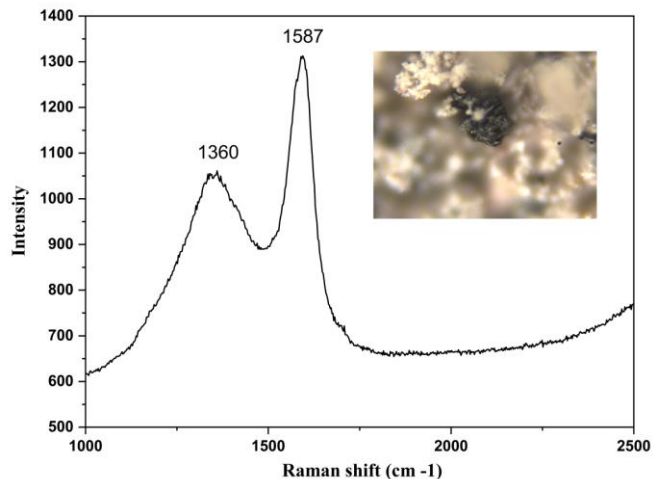


Figure 6 Raman spectrum of a carbonaceous particle isolated from fermented grape pomace ash, exhibiting characteristic D ($\sim 1350\text{ cm}^{-1}$) and G ($\sim 1590\text{ cm}^{-1}$) bands typical of disordered sp^2 carbon structures.

From a mechanistic perspective, the coexistence of disordered carbon and copper species provides a structurally consistent explanation for the partial reduction of Cu^{2+} species inferred from UV Vis analysis. Such carbon-rich microdomains may transiently act as reducing environments during thermal treatment.

Distinct Raman modes attributable exclusively to crystalline CuO were not clearly resolved, which is consistent with peak overlap in XRD and suggests fine dispersion or structural association of copper within the phosphate-carbonate matrix.

3.4.4. Structural Implications in View of Application Potential

The combined spectroscopic results refine the structural model derived from XRF and XRD analyses and provide additional insight into the physicochemical state of the material.

The ash is composed of a calcium phosphate-carbonate mineral framework incorporating dispersed copper species and residual carbon domains formed during thermal transformation. The identification of apatite-type phosphate phases with partial carbonate substitution suggests a structurally stable but potentially moderately reactive mineral matrix. The presence of disordered carbon indicates incomplete combustion and local redox heterogeneity, while UV Vis evidence of metallic Cu^0 nanoparticles confirms that partial reduction of copper species occurred during thermal processing.

From a materials perspective, this structural configuration directly influences the potential behavior of the ash under environmental or technological conditions. Phosphate bonding environments, carbonate substitution, copper speciation, and residual carbon content are expected to govern dissolution kinetics,

redox interactions, nutrient release profiles, trace metal mobility, and reactivity in alkaline systems.

Accordingly, the structural features identified through optical and vibrational spectroscopy provide the physicochemical basis for evaluating the technically plausible application pathways discussed in the following section.

3.5. Potential application of fermented grape pomace ash

3.5.1. Agricultural application as fertilizer or soil amendment

The physicochemical profile of the fermented grape pomace ash, characterized by high $\text{CaO-K}_2\text{O-P}_2\text{O}_5$ contents, moderate MgO and SiO_2 fractions, a partially amorphous phase assemblage, and elevated copper concentration, enables several technically plausible application pathways. However, each route requires application-specific validation, particularly with respect to solubility, leaching behaviour, and long-term stability.

The high concentrations of potassium (29.7 wt.% K_2O) and phosphorus (16.3 wt.% P_2O_5), combined with Ca and Mg, position fermented grape pomace ash as a potential multi-nutrient mineral fertilizer. Potassium is predominantly present in soluble or partially soluble phases (e.g., sulphates), whereas phosphorus is largely associated with calcium phosphate phases, including hydroxyapatite. This mineralogical form suggests a relatively slow P-release profile, potentially advantageous for sustained nutrient supply and reduced leaching compared to highly soluble phosphate fertilizers. Calcium and magnesium may contribute to soil pH correction, particularly in acidic soils, due to the presence of free lime and carbonate phases. The neutralizing potential of the ash should therefore be quantified via acid-base titration and compared with conventional liming agents. A critical constraint, however, is the elevated copper content (>2 wt.% CuO equivalent). While copper is an essential micronutrient, excessive accumulation may result in phytotoxicity and soil contamination, particularly under repeated application

3.5.2. CO_2 sequestration and mineral carbonation

The high CaO content (34.9 wt.% before washing and 45.6 wt.% after washing) indicates a substantial theoretical carbonation capacity of the fermented grape pomace ash. Free lime, together with other alkaline oxides such as MgO and K_2O , can react with atmospheric or concentrated CO_2 to form thermodynamically stable carbonate phases. The simultaneous presence of CaO and CaCO_3 in the analyzed material suggests that partial spontaneous carbonation has already occurred during cooling in the combustion chamber and subsequent storage under ambient conditions.

Under controlled conditions, mineral carbonation of fermented grape pomace ash could enable permanent CO_2 fixation through the conversion of reactive oxides into stable carbonates. This transformation would simultaneously stabilize free lime, reducing the risk of volumetric instability, and lower the overall alkalinity of the material, potentially decreasing the mobility of trace metals, including copper. The carbonation process may therefore function both as a carbon sequestration pathway and as a chemical stabilization strategy.

3.5.3. Use in cementitious and alkali-activated materials

The mineralogical and chemical characteristics of the fermented grape pomace ash indicate that it may be incorporated into cementitious systems either as a supplementary mineral additive at low replacement levels or as a precursor component in alkali-activated and hybrid binders. This potential derives from several intrinsic features of the material. The XRD pattern reveals a significant amorphous fraction, evidenced by the diffuse halo in the $25\text{--}35^\circ 2\theta$ range, which may provide pozzolanic or alkali-activation reactivity. The presence of free CaO and calcite contributes to inherent alkalinity, while moderate SiO_2 and Al_2O_3 contents offer a minimal aluminosilicate framework. After grinding, the ash exhibits

a fine particulate morphology that may support filler effects and particle packing improvement in composite systems.

In Portland cement-based matrices, fermented grape pomace ash would be expected to function as a filler and as reactive pozzolan. The elevated phosphate content, however, introduces potential interactions with early hydration processes but hydroxyapatite is relative stable in alkaline conditions. For this reason, detailed studies and setting time measurements, are necessary to quantify any modification of hydration behavior.

In alkali-activated and geopolymers systems fermented grape pomace ash may contribute additional calcium for C–A–S–H-type gel formation. The amorphous fraction could display partial dissolution under highly alkaline activation. The relatively high P content may again influence gel chemistry in Ca-rich systems, and its incorporation into the reaction products should be clarified using spectroscopic or microstructural techniques.

A significant limitation of the untreated ash is the presence of soluble sulfates and chlorides. These components may increase the risk of reinforcement corrosion, promote secondary ettringite formation under favorable conditions, and potentially affect dimensional stability and long-term durability. The washing procedure substantially reduces SO_3 , Cl, and K_2O contents, demonstrating that pre-treatment effectively lowers the concentration of soluble salts and enhances compatibility with reinforced cementitious systems.

3.5.4. UV–Vis diffuse reflectance analysis

Copper is recognized as a strategic and critical raw material within the European Union due to its central role in electrical infrastructure, renewable energy technologies, and electrification pathways. The relatively high copper concentration in fermented grape pomace ash (2.12 wt.% expressed as CuO) and 3.5wt.% in the washed ash, therefore represents a potential resource opportunity. The feasibility of selective recovery depends strongly on copper speciation. Spectroscopic evidence indicating the presence of metallic Cu^0 nanoparticles, in addition to oxidized Cu^{2+} species, suggests that at least part of the copper may be accessible through reductive or acidic dissolution routes. Hydrometallurgical processing, such as controlled acid leaching followed by electrochemical recovery or precipitation, could be considered as a valorization pathway. However, the economic viability of such an approach would depend on several interrelated factors, including the fraction of extractable copper relative to total content, the efficiency and selectivity of the leaching process in the presence of high Ca and P concentrations, the energy and reagent demand, and the overall scale of ash generation.

An alternative strategy is direct functional utilization of the copper-bearing ash without prior extraction. Copper species, including both Cu^0 nanoparticles and Cu^{2+} ions, are widely recognized for their bactericidal and fungicidal properties [23]. In this context, fermented grape pomace ash could serve as an antimicrobial additive in mineral matrices. One practical application may involve incorporation into lime-based formulations for winter treatment of fruit tree's trunks, where copper-based compounds are traditionally employed. In addition, the ash could be explored as a functional component in antimicrobial mineral coatings or as a filler in cementitious composites designed for hygienic or high-contact surfaces.

4. Conclusions

Fermented grape pomace ash derived from brandy production represents a chemically complex Ca–K–P-rich biomass ash characterized by pronounced alkalinity, elevated phosphorus content, and a notable concentration of copper. A water-soluble fraction of 17.1 wt.% indicates the presence of mobile salts (mostly arcanite), which govern leaching behaviour and define both functional reactivity and environmental risk.

Accordingly, this material should be regarded not as a waste residue but as a multifunctional secondary raw resource, with prospective applications in soil amendment, mineral CO_2 sequestration, and incorporation into cementitious or alkali-activated binder systems, subject to appropriate environmental and performance validation.

Acknowledgements: This work has been carried out in the framework of the National Science Program "Critical and strategic raw materials for a green transition and sustainable development", approved by the Resolution of the Council of Ministers № 508/18.07.2024 and funded by the Ministry of Education and Science (MES) of Bulgaria. We would like to express our gratitude for the technical support to programme "Research, Innovation and Digitalisation for Smart Transformation" 2021–2027, funded by the European Union, Project BG16RFPR002-1.014-0007 "Center for Competence PERIMED-2".

5. References:

- Miranda, M.; Arranz, J.; Román, S.; Rojas, S.; Montero, I.; López, M.; Cruz, J. Characterization of grape pomace and pyrenean oak pellets. *Fuel processing technology* **2011**, *92*, 278-283.
- Pereira, P.; Palma, C.; Ferreira-Pêgo, C.; Amaral, O.; Amaral, A.; Rijo, P.; Gregório, J.; Palma, L.; Nicolai, M. Grape pomace: A potential ingredient for the human diet. *Foods* **2020**, *9*, 1772.
- Pop, I.; Pascariu, S.M.; Simeanu, D.; Radu-Rusu, C.; Albu, A. Determination of the chemical composition of the grape pomace of different varieties of grapes. *Scientific Papers-Animal Science Series: Lucrariitnificie-Seria Zootehnie* **2015**, *63*, 76-80.
- Valiente, C.; Arrigoni, E.; Esteban, R.; Amado, R. Grape pomace as a potential food fiber. *Journal of Food Science* **1995**, *60*, 818-820.
- Mohamed Ahmed, I.A.; Özcan, M.M.; Al Juhaimi, F.; Babiker, E.F.E.; Ghafoor, K.; Banjanin, T.; Osman, M.A.; Gassem, M.A.; Alqah, H.A. Chemical composition, bioactive compounds, mineral contents, and fatty acid composition of pomace powder of different grape varieties. *Journal of Food Processing and Preservation* **2020**, *44*, e14539.
- Mortari, D.; Perondi, D.; Rossi, G.; Bonato, J.; Godinho, M.; Pereira, F. The influence of water-soluble inorganic matter on combustion of grape pomace and its chars produced by slow and fast pyrolysis. *Fuel* **2021**, *284*, 118880.
- Moço, A.; Costa, M.; Casaca, C. Ash deposit formation during the combustion of pulverized grape pomace in a drop tube furnace. *Energy conversion and management* **2018**, *169*, 383-389.
- Vassilev, S.V.; Baxter, D.; Vassileva, C.G. An overview of the behaviour of biomass during combustion: Part I. Phase-mineral transformations of organic and inorganic matter. *Fuel* **2013**, *112*, 391-449.
- Nikolov, A.; Kostov, V.; Petrova, N.; Tsvetanova, L.; Vassilev, S.V.; Titorenkova, R. Sunflower Shells Biomass Fly Ash as Alternative Alkali Activator for One-Part Cement Based on Ladle Slag. *Ceramics* **2025**, *8*, 79.
- Vassilev, S.V.; Vassileva, C.G. Water-soluble fractions of biomass and biomass ash and their significance for biofuel application. *Energy & Fuels* **2019**, *33*, 2763-2777.
- Oliveira, M.; Teixeira, B.M.; Toste, R.; Borges, A.D. Transforming wine by-products into energy: Evaluating grape pomace and distillation stillage for biomass pellet production. *Applied Sciences* **2024**, *14*, 7313.
- Kalembkiewicz, J.; Galas, D.; Sitarz-Palczak, E. The physicochemical properties and composition of biomass ash and evaluating directions of its applications. *Polish Journal of Environmental Studies* **2018**, *27*, 2593-2603.
- Machado, A.R.; Voss, G.B.; Machado, M.; Paiva, J.A.; Nunes, J.; Pintado, M. Chemical characterization of the cultivar 'Vinhão'(Vitis vinifera L.) grape pomace towards its circular valorisation and its health benefits. *Measurement: Food* **2024**, *15*, 100175.

14. Wang, J.; Ma, T.; Wei, M.; Lan, T.; Bao, S.; Zhao, Q.; Fang, Y.; Sun, X. Copper in grape and wine industry: Source, presence, impacts on production and human health, and removal methods. *Comprehensive Reviews in Food Science and Food Safety* **2023**, *22*, 1794-1816.
15. Nikolov, A.; Kostov-Kytin, V.; Tarassov, M.; Tsvetanova, L.; Lazarova, H.; Tasheva, T. Products of carbonation of cement kiln dust. *Review of the Bulgarian Geological Society* **2024**, *85*, 163-166.
16. Kandikonda, R.; Murugadoss, G.; Venkatesh, N.; Subbaraj, S.S.V.; Palani, D.; Thota, S.; Rajaboina, R.K.; Divi, H.; Dhayalan, M.; Phanumartwiwath, A. Redox-driven synthesis of stable copper nanoparticles via metal displacement and their application in organic dye degradation. *Materials Advances* **2025**, *6*, 9575-9589.
17. Rehman, I.; Bonfield, W. Characterization of hydroxyapatite and carbonated apatite by photo acoustic FTIR spectroscopy. *Journal of materials science: materials in Medicine* **1997**, *8*, 1-4.
18. Grunenwald, A.; Keyser, C.; Sautereau, A.-M.; Crubézy, E.; Ludes, B.; Drouet, C. Revisiting carbonate quantification in apatite (bio) minerals: a validated FTIR methodology. *Journal of archaeological science* **2014**, *49*, 134-141.
19. Apfelbaum, F.; Diab, H.; Mayer, I.; Featherstone, J. An FTIR study of carbonate in synthetic apatites. *Journal of inorganic biochemistry* **1992**, *45*, 277-282.
20. Stoch, A.; Jastrzębski, W.; Brożek, A.; Trybalska, B.; Cichocińska, M.; Szarawara, E. FTIR monitoring of the growth of the carbonate containing apatite layers from simulated and natural body fluids. *Journal of Molecular Structure* **1999**, *511*, 287-294.
21. Baldassarre, F.; Altomare, A.; Mesto, E.; Lacalamita, M.; Dida, B.; Mele, A.; Bauer, E.M.; Puzone, M.; Tempesta, E.; Capelli, D. Structural characterization of low-Sr-doped hydroxyapatite obtained by solid-state synthesis. *Crystals* **2023**, *13*, 117.
22. Penel, G.; Leroy, G.; Rey, C.; Bres, E. MicroRaman spectral study of the PO₄ and CO₃ vibrational modes in synthetic and biological apatites. *Calcified tissue international* **1998**, *63*, 475-481.
23. Nikolov, A.; Dobрева, L.; Danova, S.; Miteva-Staleva, J.; Krumova, E.; Rashev, V.; Vilhelmova-Ilieva, N. Natural and modified zeolite clinoptilolite with antimicrobial properties: A review. *Acta Microbiologica Bulgarica* **2023**, *39*, 147-161.